SPACE-CHARGE EFFECTS OF TRANSITION CROSSING IN THE FERMILAB BOOSTER

King-Yuen Ng
Fermi National Accelerator Laboratory†, *Batavia, IL 60510*

I. INTRODUCTION

The area of a typical Fermilab booster bunch is roughly constant before transition but increases abruptly afterward[1] (Fig. 1). The mountain-range plots of Fig. 2 reveal quadrupole bunch oscillations after transition. This increase in bunch area may not be a result of microwave growth but is due to the mismatch of the RF bucket introduced by space-charge effects. The space-charge force increases the energy of particles at the front of a bunch and decreases it at the rear. Thus, below transition, the bunch is longer than if space-charge were absent and is shorter above transition (Fig. 3). After transition the bunch length will have to be shortened in order to fit the bucket. But, in doing so, it will generally overshoot (become too short) and therefore oscillate about the equilibrium length (Fig. 4).

II. EQUATIONS OF MOTION

Assume that the RF voltage V_{RF} is linearized, the RF phase φ_0 (or $\pi-\varphi_0$) are held constant over a time period including point of transition, and the frequency-flip parameter per unit

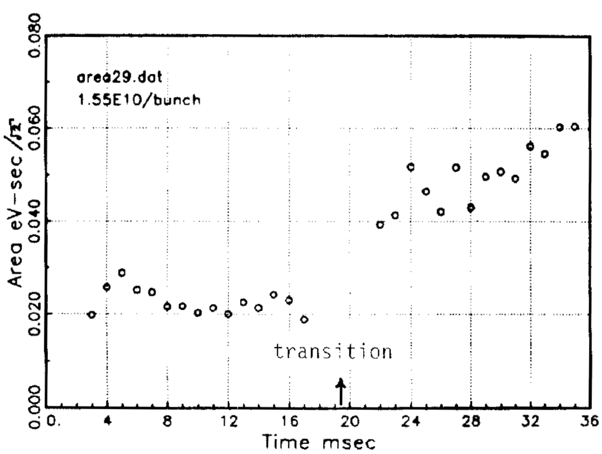

Figure 1: Longitudinal booster bunch area.

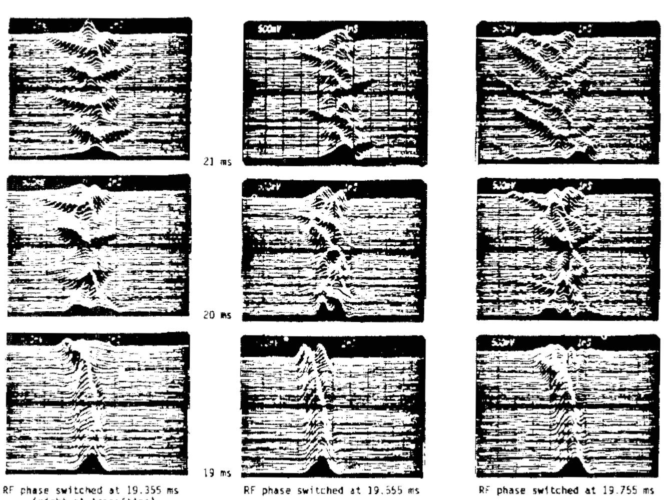

Figure 2: Mountain-range plots of a bunch across transition.

---

†Operated by the Universities Research Association, Inc., under contract with the U. S. Department of Energy.

Fig. 3

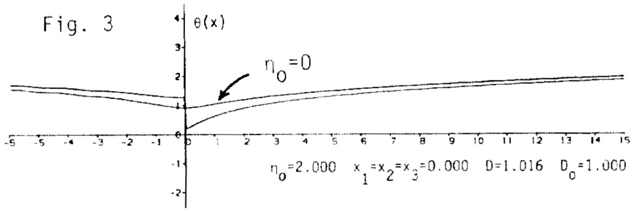

Fig. 4

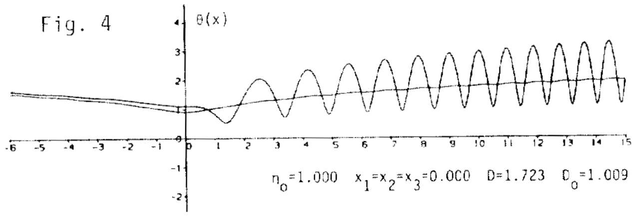

Fig. 5

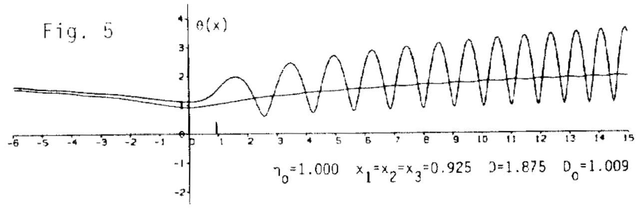

Fig. 6

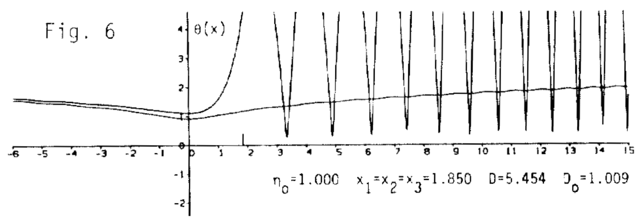

particle energy η/E varies as a linear function of time. The normalized bunch half length $\theta(x)$ of a *parabolic* bunch and its canonical momentum $P(x)$ evolve as functions of the normalized time x according to[2]

$$\frac{d\theta}{dx}=xP. \tag{1}$$

$$\frac{dP}{dx}=-sgn\,[(x-x_1)(x-x_2)(x-x_3)]\,\theta-\frac{0.7723\eta_0}{\theta^2}+\frac{x}{\theta^3}. \tag{2}$$

The real time is x multiplied by the characteristic time

$$T=\left[\left(\frac{\gamma_t^4}{2\dot{\gamma}_t h\omega_\infty^2}\right)\left(\frac{2\pi E_0}{eV_{RF}\,|\cos\varphi_0|}\right)\right]^{\frac{1}{2}}, \tag{3}$$

where $E_0=m_pc^2$ is the energy of the proton at rest, ω_∞ the angular revolution frequency of a particle around the ring travelling with the velocity of light c, h the RF harmonic, $\dot{\gamma}_t=eV_{RF}\sin\varphi_0\omega_\infty\beta_t/2\pi E_0$, and $\beta_t c$ the particle velocity at transition. Note that T depends on V_{RF} and φ_0 only and is independent of the bunch intensity. The characteristic time T is the time around transition when the evolution is not adiabatic. The symbols x_1, x_2, x_3 in Eq. (2) allow for three possible time moments when the RF phase φ_0 is switched to $\pi-\varphi_0$, then back to φ_0 and to $\pi-\varphi_0$ again; $x=0$ is right at transition. The normalized half bunch length θ is related to the true half bunch length $\hat{\theta}$ in RF radians by $\hat{\theta}=(3/\pi)^{1/2}A\theta$, where $A=(2\dot{\gamma}_t S/3E_0)^{1/2}(h\omega_\infty T/\gamma_t^2)$. The normalized half bunch height $p(x)=\sqrt{P^2+\theta^{-2}}$ is related to the maximum half bunch height $\Delta\hat{E}/E$ by

$$\frac{\Delta\hat{E}}{E}=\left(\frac{3}{\pi}\right)^{\frac{1}{2}}\left(\frac{TA}{\gamma_t}\right)p(x), \tag{4}$$

CH2387-9/87/0000-1129 $1.00 © IEEE
PAC 1987

where $\Gamma = (eV_{RF}\beta_t^2\gamma_t^4\cos^2\varphi_0/4\pi h E_0 \sin\varphi_0)^{1/3}$.

The total rate of energy increase can be written as

$$\dot{E} = \frac{eV_{RF}\omega \cos\varphi_0}{2\pi}(1+\eta_{sc})\,\Delta\varphi. \tag{5}$$

In above, aside from the RF, $\eta_{sc} = \eta_0(\hat{\theta}_0/\hat{\theta})^3$ represents the space-charge contribution, where $\omega = \beta_t\omega_\infty$, $\hat{\theta}_0$ is $\hat{\theta}$ at transition *without* space charge, and for N/h particles per bunch,

$$\eta_0 = \frac{1}{2}\left(\frac{3}{2}\right)^{\frac{1}{2}}\left(\frac{\pi}{\Gamma(\frac{2}{3})}\right)^3\left(\frac{r_p N g_0 E_0^2}{hcS^{3/2}}\right)\left(\frac{2\pi}{eV_{RF}\sin\varphi_0\omega}\right)^{\frac{1}{2}}, \tag{6}$$

with $r_p = 1.5347\times10^{-16}$ cm, the classical proton radius and $g_0 = 2\ln(b/a)+1$ the familiar space-charge geometric factor. This space-charge parameter η_0 is the only parameter in the equations of motion (1) and (2), which are therefore universal for all machines.

A distortion parameter D, defined as the square root of the ratio of the maximum to minimum bunch lengths, is introduced to measure the elongation of the bunch or the distortion from the equilibrium bunch shape. In each plot below, the D quoted is the value at $x = 15$ and D_0 the value without space charge.

III. COMPARISON WITH MEASUREMENTS

The RF phase was flipped right at transition, 0.2 ms and 0.4 ms after transition respectively in the three measurements. The corresponding theoretical predictions are shown in Figs. 4, 5, 6. Each successive trace represents a lapse of 10 turns. Total number of particles is $N = 1.30\times10^{12}$. RF voltage $V_{RF} = 763$ kV, RF phase $\varphi_0 = 53.6°$, RF harmonic $h = 84$, bunch area $S = 0.025$ eV-sec, $\gamma_t = 5.373$, and revolution frequency $\omega_\infty = 3.972\times10^6$ Hz. Thus, $\dot{\gamma}_t = 406.5$ sec^{-1} and $T = 0.216$ ms. The space-charge parameter is $\eta_0 = 0.2183\,g_0 \sim 1$ assuming that $g_0 \sim 4.5$. The true half bunch length $\hat{\theta}$ is related to the normalized half length θ by $\hat{\theta} = 0.2073\,\theta$.

Table 1 compares the mountain-range plot with theoretical predictions when the transition takes place at $x_1 = x_2 = x_3 = 0$. In general, the agreement of experiment with theory is quite good although the experimental oscillation periods are consistently 8% bigger and the experimental half bunch lengths are smaller. The discrepancy is due to the linearization of the RF force in Eqs. (1) and (2). In fact, the elongated bunch fills up a very large part of the accelerating bucket. This also explains why filamentation was observed just a couple of synchrotron oscillations ($\sim$ 2.7 ms) after transition. We note that the positions of the extrema are not sensitive to η_0 at all.

When the RF phase is flipped at $x_1 = x_2 = x_3 = 0.2/0.216 = 0.925$, the experimental traces show an apparent split in the bunch just after transition. This is not shown in the numerical solution of Fig. 5. This may be due to modification of the RF potential by other effects (for example, wall impedance) other than space charge or microwave growth discussed in the next section. Since the origin of the split is not clear, no comparison with theory has been attempted.

	Experimental			Theoretical		
	trace no.	time (ms)	half length (RF rad)	x	xT (ms)	half length (RF rad)
transition	23	0.00	0.24	0.00	0.00	0.23
1st min.	43	0.32		1.40	0.30	
1st max.	60	0.60	0.42	2.56	0.55	0.52
2nd min.	72	0.79		3.40	0.73	
2nd max.	83	0.97	0.49	0.42	0.91	0.59
3rd min.	94	1.14		4.91	1.06	
3rd max.	104	1.30	0.53	5.59	1.21	0.64
4th min.	113	1.45		6.21	1.34	
4th max.	122	1.59	0.56	6.82	1.47	0.72

Table 1: Bunch lengths comparison for first performance.

	Experimental			Theoretical		
	trace no.	time (ms)	half length (RF rad)	x	xT (ms)	half length (RF rad)
transition	23	0.00	0.23	0.00	0.00	0.23
1st max.	60	0.60	0.62	2.54	0.53	1.40
1st min.	72	0.79		3.35	0.72	
2nd max.	84	0.98	0.72	4.17	0.90	1.59
2nd min.	95	1.16		4.89	1.06	
3rd max.	106	1.34	0.72	5.59	1.21	1.64
3rd min.	115	1.48		6.26	1.35	
4th max	124	1.63	0.72	6.85	1.48	1.85

Table 2: Bunch lengths comparison for third performance.

For the third mountain range, the RF phase is flipped at $x_1 = x_2 = x_3 = 0.4/0.216 = 1.85$. The experimental results exhibit no first minimum which agree with the theoretical predictions in Table 2. Again the positions of maxima and minima are consistently bigger for the experimental results and this is due to a tight bucket which gives a lower average oscillation rate. The predicted maximum half lengths are too big. Of course, this is due mostly to the linearization of the RF force. However, they are very sensitive to the time at which the RF phase is switched. An earlier switch will lower these maxima by very much. Since the agreement between experimental measurements and theory, at least for the first and third performances, we may conclude that the growth in bunch area across transition is due mostly to space-charge effects which lead to bunch tumbling inside the bucket and eventual filamentation.

IV. MICROWAVE INSTABILITY

Above transition, space-charge force inevitably drives microwave instability. However, with the assumption of a *linearized* RF, the bunch area is conserved and therefore microwave growth has not been included. Usually the worst growth will appear only during the first few units of the characteristic time T. Figures 7, 8, 9 show the energy half spreads when the RF phases are switched at $x = 0.0, 0.93$ and 1.85 (or $t = 0.0, 0.20, 0.40$ ms) respectively. Both Figs. 7 and 9 display, during the first

Fig. 7

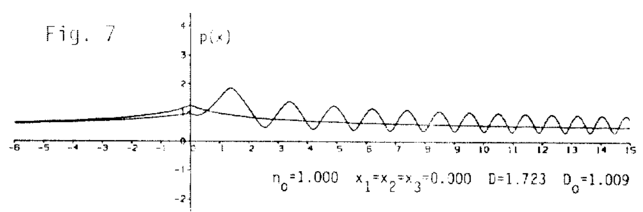

Fig. 8

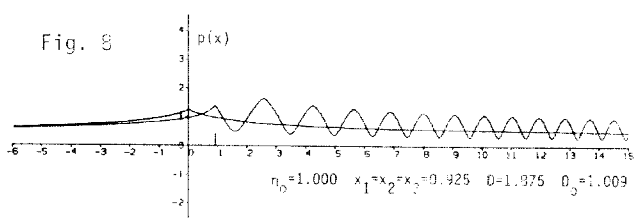

Fig. 9

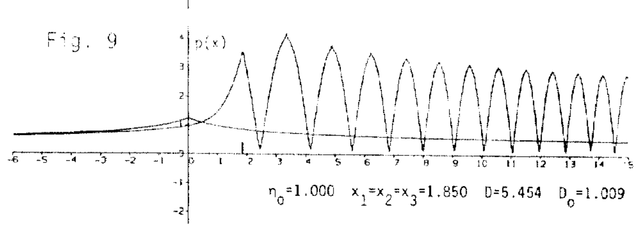

few units of T, energy spreads which are much bigger than that when there is no space charge. As a result, the oscillations after transition do lower the growth of the microwave amplitudes and therefore the bunch area, although we do not know how to relate the two growths. When the RF phase is switched at $x = 0.93$ (or $t = 0.20$ ms), we do not see the big energy-spread peak just after transition (Fig. 8). As a result, the microwave growth is expected to be bigger. This may explain why the experimental data shows a split bunch (Fig. 2).

V. CURES OF BUNCH TUMBLING

Here, we discuss three methods to cure bunch tumbling. Sorenssen[2] suggested switching the RF phase back and forth three times. The idea is: after switching the phase from φ_0 to $\pi - \varphi_0$ at $x_1 = 0$, the bunch tries to adjust itself to fit the configuration of shorter bunch length (Fig. 4). At some time x_2 before the overshoot, the phase is switched from $\pi = \varphi_0$ to φ_0. The bunch is then at an unstable fixed point and it will try to lengthen. Then, the phase is switched back to $\pi - \varphi_0$ at x_3 so chosen that the bunch lengthening between this interval will cancel the overshoot thus damping out the oscillations and eventual filamentation.

With $\eta_0 = 1$, we find a set of time $x_2 = 0.688$ and $x_3 = 1.289$ that will cancel the overshoot. The distortion factor is reduced from the original $D = 1.72$ to $D = 1.03$ (Fig. 10).

However, this method has not been successful on the CERN PS. The reasons may be:

(1) The best moment to damp the oscillations is to cancel the first overshoot in order to avoid filamentation. However, this will eliminate the first broad peak of the energy spread also (Fig. 11) and lead to a bigger microwave growth.

(2) The timings x_2 and x_3 depend critically on the size of the space-charge force. Since η_0 depends on the bunch intensity which varies in each injection and the timings x_1, x_2 and x_3 have to be accurate up to $\sim \pm 1\mu s$, it is nearly impossible to maintain a correct set of switching times.

A feed-back device can be used to damp out the quadrupole motion of the bunch. However, filamentation begins just after about four oscillations or $\sim$ 1.5ms. This implies that the damping must be done within this short period which poses some technical difficulty.

The third method is γ_t jump. As a bunch is approaching transition from below, if the transition gamma γ_t is suddenly changed to a new value below the instantaneous γ of the bunch, the bunch will not see transition at all. This method is nice because the bunch is never very near to transition, so microwave growth can be avoided to a very large extent. Secondly, away from transition, the equilibrium bunch length is not so much different from that if space charge is absent as shown in Fig. 3. Therefore, oscillations after the transition jump will generally be rather small. Last of all, γ_t can actually be changed rather easily by pulsing some quadrupole magnets in a special way.

For the case $\dot\gamma = 406.5\,\text{sec}^{-1}$ near transition and $T = 0.216$ ms, a transition jump of 10 units in x corresponds to γ_t changing by roughly 0.9. We can solve the equations of in Section II by letting $x_2 = 0, x_1$ negative, x_3 positive but $x_3 - x_1 = 10$. As soon as the integration reaches $x = x_1$, we set $x = x_3$.

As is shown in Fig. 3, the equilibrium bunch length is bigger than the bunch length without space charge below transition but smaller than the bunch length above transition. In order that the equilibrium bunch lengths before and after transition will match so as to reduce eventual oscillations as much as possible, it is beneficial to have $|x_1| < |x_3|$ or to have the transition jump performed when *the energy of the bunch is closer to the old transition energy than the new one.* The results of some computations are listed in Table 3. It is obvious that the best jump should be performed at $x_2 = -0.4.0$ and $x_3 = 6.0$ which appear to depend very weakly on the space-charge strength. Translating to the actual time units, if we want to perform a transition jump from $\gamma_t = 5.37$ to 4.47, the best time to make the jump is when the bunch is $4.0 \times 0.216 = 0.86$ ms before the original transition time or when the bunch has a γ of $5.37 - 0.86 \times 10^{-3} \times 406.5 = 5.02$.

Fig. 10

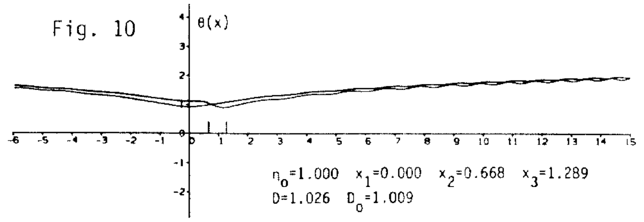

Fig. 11

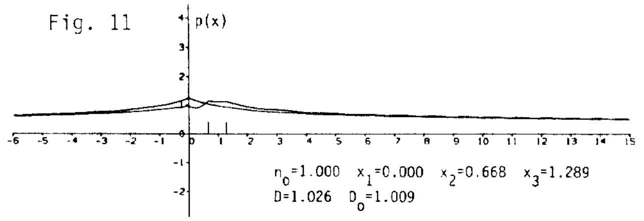

VI. CONCLUSION

We have studied the space-charge effects on a bunch across transition. Since the RF potential has been linearized, the bunch area becomes a constant and no microwave growth has been included. However, the tumbling of the bunch after transition agrees very well with the measurements indicating that impedance of other sources and microwave instability are of minor importance here. γ_t jump has been investigated in order to cure the bunch tumbling. This is the most ideal method to reduce tumbling. We find that, in order to achieve the best tumbling suppression, the timing of the transition jump should be tuned to a point where the energy of the bunch is closer to the old transition energy than the new one.

		Distortion D		
x_1	x_3	$\eta_0 = 1.00$	$\eta_0 = 0.75$	$\eta_0 = 1.25$
0.0	0.0	1.72	1.55	1.89
-5.0	5.0	1.11	1.08	1.14
-4.5	5.5	1.07	1.05	1.10
-4.0	6.0	1.03	1.02	1.05
-3.5	6.5	1.05	1.07	1.02
-3.0	7.0	1.09	1.12	1.06

Table 3: Distortions for a transition jump of $\Delta\gamma_t \sim 0.9$.

References

[1] J. Crisp, Fermilab Director Review (1986).

[2] A. Sorenssen, CERN Report MPS/Int. MU/EP 67-2 also Particle Accelerators **6**, 141 (1975).